Journal of Chromatography, 357 (1986) 11–32
Elsevier Science Publishers B.V., Amsterdam — Printed in The Netherlands

CHROM. 18 425

EXAMINATION OF THE THERMODYNAMIC AND KINETIC CHARACTERISTICS OF MICROPARTICULATE AFFINITY CHROMATOGRAPHY SUPPORTS

APPLICATION TO CONCANAVALIN A

AMY J. MULLER*
AT&T Bell Laboratories, 600 Mountain Avenue, Murray Hill, NJ 07974 (U.S.A.)
and
PETER W. CARR
University of Minnesota, Department of Chemistry, 207 Pleasant St SE, Minneapolis, MN 55455 (U.S.A.)
(First received August 27th, 1985; revised manuscript received December 18th, 1985)

SUMMARY

The relatively new technique of high-performance liquid affinity chromatography (HPLAC) has been plagued by very large plate heights. Here we show that the large plate heights observed in the concanavalin A (Con A) HPLAC system arise from the sluggish chemical kinetics of the Con A–sugar interaction, and that other mass transfer terms contribute much less to the observed plate height. The rate parameters for the association and dissociation of various sugar derivatives from silica-bound Con A are chromatographically determined. The effects of isotherm non-linearity on both the thermodynamic and kinetic properties of immobilized Con A are described. The enhancement effect of mobile phase competing sugar on the kinetics of the immobilized Con A–sugar interaction is investigated in detail, and possible reasons for this effect are proposed.

INTRODUCTION

Recent studies in the field of high-performance liquid affinity chromatography (HPLAC) have suggested that the limits of this new technique may be set by the sluggish chemical kinetics of the immobilized ligand–solute interaction[1–5]. The sluggish kinetics may lead to intolerably wide peaks in some cases, or in other cases, seemingly irreversible solute adsorption. In a previous paper, we presented an experimental method for the chromatographic determination of heterogeneous rate constants in HPLAC and demonstrated that for the concanavalin A (Con A) HPLAC system, the heterogeneous dissociation rate constant of the monovalent carbohydrate, *p*-nitrophenyl-α-D-mannoside (pNp-mannoside), from immobilized Con A is significantly lower than the corresponding solution phase value[6].

We have also previously demonstrated that, unlike the kinetic parameters, the

0021-9673/86/$03.50

thermodynamic parameters of the interaction are largely unaffected by immobilization and that biospecificity is preserved. These studies are extended here to include other carbohydrate solutes and to explore the effects of isotherm non-linearity on the thermodynamic and kinetic properties of immobilized Con A. We will present further evidence indicating that the large plate heights observed in this HPLAC system are the result of slow chemical kinetics and are definitely not mass transfer related. In addition, the enhancement effect of mobile phase competing sugar on the heterogeneous dissociation rate constant of the injected sugar is investigated in more detail, and possible explanations for this effect are proposed. The complex effect of isotherm non-linearity on the apparent dissociation rate constants, with and without mobile phase competing sugar, is also discussed.

The method used to determine the heterogeneous rate constants in HPLAC is described fully in a previous publication[6] and briefly outlined here. The method is based on the general plate height equation developed by Horváth and Lin[7] and shown below:

$$H_{\text{tot}} = H_{\text{disp}} + H_{\text{ext diff}} + H_{\text{int diff}} + H_{\text{kinetic}} \tag{1}$$

This equation allows one to separate the total observed plate height into contributions from four physically independent processes. The first three terms of eqn. 1 represent the non-kinetic contributions to plate height and describe the peak broadening processes occurring in the mobile phase, H_{disp}, at the particle boundary, $H_{\text{ext diff}}$, and within the pores, $H_{\text{int diff}}$. Each of these three non-kinetic contributions can be expressed as functions of chromatographic and structural packing parameters as shown in refs. 7 and 8. For our purposes, the most significant aspect of the non-kinetic contributions is that each of these three terms is proportional to some power of the particle diameter.

The last term of eqn. 1, H_{kinetic}, is given by

$$H_{\text{kinetic}} = \frac{2k'u_e}{(1 + k')^2 k_d(1 + k_0)} = \frac{2k'^2u_e}{(1 + k')^2 \varphi k_a(1 + k_0)} \tag{2}$$

and represents the peak broadening due to the chemical binding and debinding of the solute at the binding site of the immobilized ligand. In essence, the first three terms of eqn. 1 wholly represent the processes involved in transporting the solute to the interior surface of the particle, while the final term describes the chemical association/dissociation process. In eqn. 2, u_e is the interstitial linear velocity, k' is the solute's capacity factor, k_0 is the intraparticle to interstitial void volume and φ is the phase ratio (moles of bioactive sites expressed with the volume of mobile phase in the column). Similarly, k_a and k_d are the association and dissociation rate constants, respectively. Note that H_{kinetic} is independent of particle diameter as one would expect for a process confined solely to the interior particle surface.

It is important at this point to understand in some detail the process represented by eqn. 2. Eqn. 2 arises from consideration of the reversible, non-instantaneous binding of the solute, S, to the covalently bound ligand, P, at the surface of the stationary phase within the pores by the simple process:

$$\text{S} + \text{P} \underset{k_d}{\overset{k_a}{\rightleftarrows}} \text{PS} \tag{3}$$

The thermodynamic equilibrium constant of the binding process is given as

$$K = \frac{c_s}{(\Lambda - c_s)\, c_m} \tag{4}$$

where c_s is the surface concentration of the complex PS, c_m is the concentration of free solute, S, in the intraparticle mobile phase and Λ is the surface concentration of all accessible ligands. In this model, it is initially assumed that the solute concentration is much less than the ligand concentration so that $\Lambda - c_s \approx \Lambda$. Furthermore, it is also assumed that no secondary equilibria are involved. In essence, the isotherm has been linearized, and thus the chromatographic characteristics are expected to be independent of solute concentration. The equilibrium constant for the process shown in eqn. 4 can be expressed in terms of the rate constants, k_a and k_d:

$$K = k_a/k_d \tag{5}$$

The capacity factor, k', is then related to the equilibrium and rate constants via the equation:

$$k' = K\varphi = k_a\varphi/k_d \tag{6}$$

Largely due to the fact that the solute binding and dissociation processes are unexplored in HPLC, Horváth and Lin chose to represent the binding kinetics at a completely homogeneous surface by the following simple kinetic expression as a first approximation:

$$\frac{\partial c_s(r)}{\partial t} = k_a c_{m,i}(r)\, \Lambda - k_d c_s(r) \tag{7}$$

where $c_s(r)$ is the surface concentration of the bound complex at radial position r in the particle and $c_{m,i}(r)$ is the solute concentration in the stagnant mobile phase inside the pore at radial position r. Solution of the partial differential equations resulting from mass balances on the solute concentrations $c_{m,i}(r)$ and c_s finally results in the expression for the kinetic plate height contribution given in eqn. 2.

In order to determine the rate constants, k_a or k_d, we first measured the total plate height for a given solute and then subtracted the non-kinetic contribution to determine the plate height due to chemical kinetics alone. From the kinetic plate height contribution, k_d and/or k_a are then easily evaluated using eqn. 2. The non-kinetic contribution to plate height was evaluated in two ways. In the first approach used to estimate $H_{\text{non-kinetic}}$, we calculated the sum of the values of H_{disp}, $H_{\text{ext diff}}$ and $H_{\text{int diff}}$ using the equations derived by Horváth and Lin[7,8] and typical literature values for the various structural packing parameters. In the second approach, we simply assumed that the total plate height for a "binding" solute would be equal to the sum of the total plate height of a "non-binding" sugar of similar chemical structure and the plate height due to slow chemical kinetics. Because $H_{\text{non-kinetic}}$ is weakly dependent on k', at least for a well-packed column and a low-molecular-weight solute, the k' values used to calculate $H_{\text{non-kinetic}}$ were those of the "binding" solutes (see Table III). The results of these two methods never differed by more than 11%[6].

Moreover, since the non-kinetic contribution to plate height only represents 20% of the total observed plate height on 10-μm particles, small differences between the two methods are unimportant.

The method described above was used to evaluate the dissociation rate constants of pNp-mannoside and pNp-glucoside as a function of concentration injected, and as a function of the concentration of mobile phase competing sugar.

EXPERIMENTAL

Materials

Concanavalin A (Con A, Type IV), *p*-nitrophenyl-α-D-mannopyranoside (pNp-mannoside), *p*-nitrophenyl-α-D-glucopyranoside (pNp-glucoside), *p*-nitrophenyl-α-D-galactopyranoside (pNp-galactoside), α-methyl-D-mannoside (MDM) and α-methyl-D-glucoside (MDG) were used as purchased from Sigma (St. Louis, MO, U.S.A.). Fractosil 500 (pore diameter 42 nm, particle diameter 40–60 μm) was obtained from E. Merck (Darmstadt, F.R.G.) and washed with concentrated nitric acid prior to use. LiChrospher 500 (Batch No. YE 496, pore diameter 50 nm, particle diameter 10 μm) was also obtained from E. Merck. γ-Aminopropyltrimethoxysilane was obtained from Silar (Scotia, NY, U.S.A.). All other chemicals were reagent grade.

Preparation of biospecific adsorbents

In most cases, the Con A was purified prior to immobilization according to the method of Cunningham *et al.*[9] to isolate the intact subunits. Con A was immobilized on both Fractosil 500 and LiChrospher 500 by the glutaraldehyde method previously described[6]. The amount of Con A bound to the silica was determined by the difference in the absorbance of the Con A supernatant solution before and after immobilization. The amount of Con A detected in the washings of the silica was also included in this determination. The amount of Con A bound to the silica (in milligrams of Con A per gram of silica) varied between 27 and 38 mg/g.

Column packing and chromatographic conditions

The 10-μm separation columns (5 cm × 0.46 cm I.D.) were slurry packed at 3000 p.s.i. using 2 m*M* MDM in distilled water as the suspending medium and the stirred upward packing method[10]. The 50-μm particles were manually slurry packed into 5 cm × 0.3 cm I.D. or 15 cm × 0.3 cm I.D. glass columns. An HPLC system comprised of a high pressure pump (Altex), an injector (Valco) fitted with a 25-μl injection loop and a UV–visible spectrophotometer (Hitachi) equipped with a 20-μl flow cell (Altex) was used. Column jackets were used and temperature control (± 1°C) was provided by a thermostatted water circulator (Haake, Model FE). The detection wavelength for the *p*-nitrophenyl sugars was 305 nm. The mobile phase used was 0.02 *M* sodium phosphate, pH 6.0 containing 0.5 *M* sodium chloride, 0.01 *M* magnesium chloride and 0.001 *M* calcium chloride. The column dead volume was measured using methanol. The data collection system consisted of a DC amplifier (Keithley Instruments) and an Apple II Plus computer equipped with the ADALAB System (Interactive Microware, State College, PA, U.S.A.).

Calculation of elution parameters

Because the chromatographic peaks obtained exhibited severe tailing, simple measurement of the volume at peak maximum could not be used as a thermodynamically valid measure of solute retention. Similarly, under these conditions, the peak width at half maximum could not be used to obtain the true peak variance using conventional Gaussian peak formulae. To circumvent these difficulties, the chromatograms were digitized on-line and the zeroth, first and second peak moments were then calculated using the digitized chromatogram and the standard definitions of the normalized central moments. The data acquisition system and the moments calculation method, including the technique used for baseline subtraction are fully explained in ref. 6.

RESULTS AND DISCUSSION

Bioselective interaction

We have previously shown that the elution order of pNp-galactoside, pNp-glucoside and pNp-mannoside on Con A-silica is the same as the relative Con A binding affinities of these sugars as determined from solution phase studies. We have developed an equilibrium model of immobilized Con A–solute binding which allows one to express the capacity factor of a given carbohydrate solute in terms of column parameters, the concentration of competing mobile phase in the column and the heterogeneous equilibrium binding constants of the injected and mobile phase sugars. This model is based solely on the equilibrium competition of S_1 and S_2 for available Con A binding sites. The form of this expression is given in eqn. 8:

$$k' = \frac{K_1 N^0_{CA}}{V_m(1 + K_2[S_2]_m)} \tag{8}$$

where K_1 and K_2 are the equilibrium binding constants of the injected and mobile phase sugars, respectively, $[S_2]_m$ is the concentration of competing sugar in the mobile phase and V_m is the volume of mobile phase in the column. N^0_{CA} is the number of moles of active Con A in the column as obtained from the measurement of the total Con A in the column (as explained in the Experimental section) and the fraction of active Con A as obtained from isotherm measurements[6]. The reciprocal form of eqn. 8 (eqn. 9) provides a convenient graphical approach to the experimental determination of K_1 and K_2:

$$\frac{1}{k'} = \frac{V_m K_2[S_2]_m}{K_1 N^0_{CA}} + \frac{V_m}{K_1 N^0_{CA}} \tag{9}$$

A plot of $[S_2]_m$ *vs.* $1/k'$ yields an intercept of $V_m/(K_1 N^0_{CA})$ on the $1/k'$ axis and a slope of $V_m K_2/(K_1 N^0_{CA})$. The value of K_2 is obtained by dividing the slope by the intercept, and K_1 can be evaluated by independently measuring V_m and N^0_{CA}.

We have previously shown that eqn. 8 is obeyed for $[S_2]_m$ greater than 0.04 mM when 1.0 mM pNp-mannoside is injected onto a Con A column containing $1.57 \cdot 10^{-7}$ mol of Con A. The binding constants used to fit the experimental data to eqn. 8, $K_1 = 1.6 \cdot 10^4\ M^{-1}$ and $K_2 = 0.76 \cdot 10^4\ M^{-1}$, were solution phase values for the interaction of MDM and pNp-mannoside with soluble Con A.

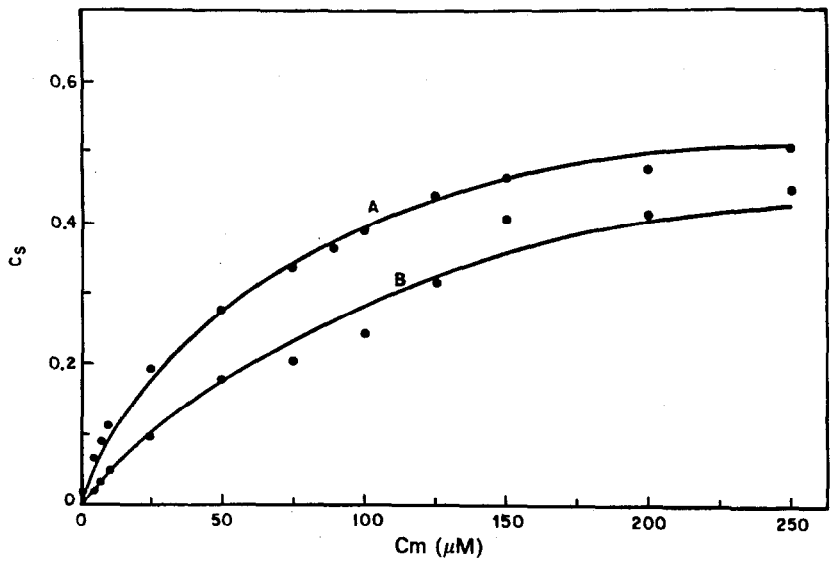

Fig. 1. Distribution isotherms of pNp-mannoside (A) and pNp-glucoside (B) on Con A-silica. Mobile phase: 0.02 *M* sodium phosphate, 0.5 *M* sodium chloride, 0.01 *M* magnesium chloride, 0.001 *M* calcium chloride, pH 6.0. Column: 5.0 cm × 0.3 cm I.D., 38 mg/g Con A (total moles of Con A = $4.2 \cdot 10^{-7}$), 50 μm, pore diameter 42 nm. Isotherm determined using the breakthrough method as described in ref. 6. C_s = fraction of Con A binding sites occupied by sugar.

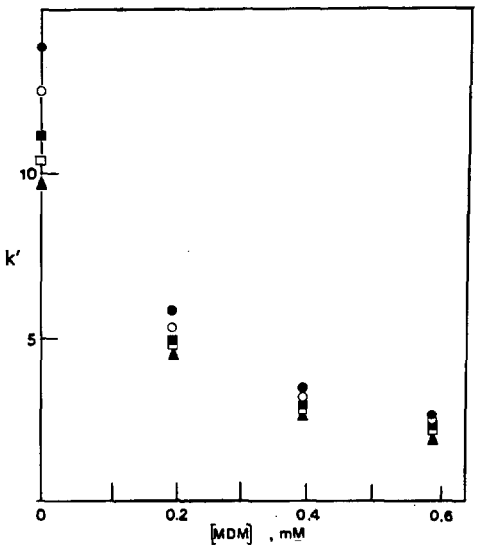

Fig. 2. Variation of *k'* (pNp-mannoside) with concentration of mobile phase competing sugar (MDM) for five different concentrations of pNp-mannoside. Column and mobile phase same as Fig. 1. Flow-rate: 1 ml/min. Sample: 25 μl of pNp-mannoside, 0.2 (●), 0.4 (○), 0.6 (■), 0.8 (□), 1.0 m*M* (▲).

However, in that experiment the concentration of pNp-mannoside injected was 1.0 mM, and the ratio of the number of moles of S_1 injected to the number of moles of active Con A binding sites was only 6.3. Since this value lies on the very non-linear portion of the distribution isotherm (see Fig. 1), we decided to explore the effect of varying the concentration of S_1 injected on the values of K_1 and K_2 obtained using eqn. 9. In this series of experiments, the value of N^0_{CA} was constant at $3.46 \cdot 10^{-7}$ mol, while the injected concentration of pNp-mannoside was varied from 0.2 to 1.0 mM. Unfortunately, the baseline noise of our system prevented exploration of the isotherm above an $N^0_{CA}/N^0_{S_1}$ ratio of 69. These results are shown in Fig. 2. In Table I, the values of K_1 and K_2 determined by linear least squares analysis of the lines obtained by plotting the data according to eqn. 9 are listed. The effect of isotherm non-linearity is clearly evident in the values given in Table I. The value of K_1 decreases monotonically from $3.5 \cdot 10^4$ to $2.3 \cdot 10^4$ M^{-1} as the concentration of S_1 injected is varied from 0.2 to 1.0 mM. These values of K_1 and K_2 are still well within the range of the reported solution phase binding constants for pNp-mannoside and MDM[11–13]. In addition, peak tailing was observed to decrease as the concentration of injected sugar was decreased providing further evidence for the existence of isotherm non-linearity.

The values of K_2 listed in Table I also decrease as the concentration of S_1 injected increases, although the percentage reduction in K_2 (20%) is less than the percentage reduction in K_1 (33%) over the S_1 concentration range of 0.2 to 1.0 mM. The reduction in K_2 may also be attributed to isotherm non-linearity, although the explanation is somewhat less intuitive than the explanation of the effect of isotherm non-linearity on K_1. As the amount of S_1 injected onto the column is increased, the number of binding sites available to S_2 is slightly decreased. The decrease in available binding sites is equivalent in this case to an increase in the amount of S_2 in the column since the important parameter is the ratio of the number of moles of S_2 to the number of moles of available binding sites. Thus, increasing the amount of S_1 in the column represents a move to a less steep region on the S_2 adsorption isotherm, and hence, a reduction in K_2.

To further evaluate the equilibrium properties of immobilized Con A, the binding constants of two additional sugars, pNp-glucoside and MDG, were determined

TABLE I

EXPERIMENTALLY DETERMINED BINDING CONSTANTS

S_1 = pNp-mannoside and S_2 = MDM. Column: 15 cm × 0.3 cm I.D., 38 mg/g Con A, 50 μm, pore diameter 42 nm. Mobile phase: 0.02 M sodium phosphate, pH 6.0, containing 0.5 M sodium chloride, 0.01 M magnesium chloride, 0.001 M calcium chloride. Flow-rate: 1.0 ml/min. Injection volume: 25 μl. K_1 and K_2 determined using eqn. 9 with V_m = 0.85 ml.

Concentration injected (mM)	$N^0_{CA} \cdot 10^7$ *(mol)*	$N^0_{CA}/N^0_{S_1}$	$K_1 \cdot 10^{-4}$ (M^{-1})	$K_2 \cdot 10^{-4}$ (M^{-1})
0.2	3.46	69	3.47	0.74
0.4	3.46	35	3.01	0.69
0.6	3.46	23	2.67	0.62
0.8	3.46	17	2.54	0.63
1.0	3.46	14	2.34	0.59

TABLE II

EXPERIMENTALLY DETERMINED BINDING CONSTANTS

S_1 = pNp-glucoside and S_2 = MDM. Column: 5 cm × 0.5 cm I.D., 27 mg/g Con A, 10 μm, pore diameter 50 nm. V_m = 0.67 ml. Concentration range of S_2 = 0 to 1.0 m*M*. All other conditions same as Table I.

Concentration injected (mM)	$N^0_{CA} \cdot 10^7$ *(mol)*	$N^0_{CA}/N^0_{S_1}$	$K_1 \cdot 10^{-4}$ (M^{-1})	$K_2 \cdot 10^{-4}$ (M^{-1})
0.01	1.85	740	0.59	0.78
0.02	1.85	370	0.60	0.81
0.10	1.85	74	0.48	0.58
0.20	1.85	37	0.46	0.57

by this method. The results for pNp-glucoside are shown in Table II. The variation in the k' value of pNp-glucoside as a function of the mobile phase concentration of MDM resulted in an experimentally determined binding constant for pNp-glucoside of (0.46–0.59) · 10^4 M^{-1}. Again, the range represents the variation of K_1 with the concentration of pNp-glucoside injected due to the isotherm non-linearity. The experimentally determined heterogeneous binding constant for pNp-glucoside is in good agreement with the solution phase values reported in the literature[14]. Comparison of the binding constants determined for pNp-mannoside and pNp-glucoside at comparable levels of $N^0_{CA}/N^0_{S_1}$ indicates that the affinity of immobilized Con A for pNp-mannoside is approximately five times greater than its affinity for pNp-glucoside. This is consistent with solution phase studies and with the relative k' values of pNp-mannoside and pNp-glucoside under conditions of no competing sugar in the mobile phase.

Because the low absorbtivity of MDG at wavelengths greater than 210 nm prohibited its use as an injected sugar, *i.e.*, $[S_1]$, the binding constant of MDG was determined by noting its effect as a mobile phase competitor on the retention of the observable injected sugar, pNp-mannoside. Only a single concentration of S_1 (0.1 m*M*, $N^0_{CA}/N^0_{S_1}$ = 160) was used in this experiment while the mobile phase concentration of MDG was varied from 0 to 2.0 m*M*. Under these conditions, the binding constant determined for MDG, 0.16 · 10^4 M^{-1}, agrees closely with the solution phase value of 0.17 · 10^4 M^{-1} determined at pH 5.6 and 25°C (ref. 15).

Although the application of eqns. 8 and 9 is complicated by the effects of isotherm non-linearity as explained above, the results presented here indicate that the relative biospecificity as well as the magnitude of the equilibrium binding constants of the Con A–carbohydrate interaction are preserved upon immobilization. Due to the fact that the isotherm is non-linear, but our method of data evaluation inherently ignores this non-linearity, the measured binding constants, K_1 and K_2, appear to be concentration dependent. If an accurate model of non-linear chromatography were available, we presume that one could generate suitable correction factors to apply to the raw moments so that the measured equilibrium constants would no longer vary with solute concentration. In short, the variations of K_1 and K_2 with injected concentration are an artifact of an inadequate model. However, the method does provide a simple means for estimating binding constants of immobilized ligands to facilitate comparison with solution phase values.

The nature of the isotherm non-linearity described here has been investigated using several approaches. Current evidence leads us to conclude that there are at least two distinct contributors to isotherm non-linearity. At moderate to high levels of sample loading, the isotherm non-linearity is dominated by statistical, *i.e.*, Langmuirian effects. At lower sample loadings, binding site heterogeneity is an important contributor to isotherm non-linearity. Scatchard analyses of the measured isotherms[6] indicate the presence of a subclass of sites with binding affinity significantly greater than the average binding site strength. Thus, at low solute concentration, a greater fraction of the total injected sugar will interact with this subclass of strong sites resulting in a larger apparent binding constant. In addition, we often observe deviations from eqn. 8 when the concentration of mobile phase competing sugar is very low (typically less than 0.05 m*M*). This deviation also implies the existence of a population of strong sites which dominate the interaction with S_1 until the concentration of S_2 is increased to a level which effectively blocks these sites from interaction with S_1. Possible sources of binding site heterogeneity include differences in the number and arrangement of the linkages between Con A and the support surface, and secondary interactions with the underlying silica surface or the glutaraldehyde molecules. For the purposes of the following discussion, it should be borne in mind that isotherm non-linearity can contribute to peak broadening.

Evaluation of kinetic parameters: concentration dependence

In our previous work, we reported that the apparent dissociation rate constant of pNp-mannoside was approximately 0.3 s^{-1}, 10–20 times lower than the reported solution phase values[11,16,17]. We now extend these studies to examine the effect of

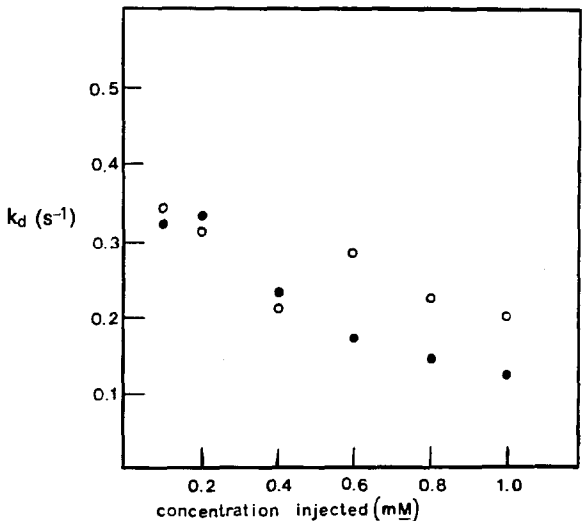

Fig. 3. Variation of the apparent dissociation rate constant of pNp-mannoside with injected concentration on 10- and 50-μm supports. ●, Apparent dissociation rate constants obtained on the 10-μm support (5.0 cm × 0.5 cm I.D., 27 mg/g Con A, pore diameter 50 nm); ○, apparent dissociation rate constants obtained on the 50-μm support (5.0 cm × 0.3 cm I.D., 38 mg/g Con A, pore diameter 42 nm). Mobile phase and flow-rate as in Fig. 2. Injection volume: 25 μl.

TABLE III

TOTAL OBSERVED PLATE HEIGHT FOR pNp-MANNOSIDE ON 10- AND 50-μm PARTICLES AND THE NON-KINETIC CONTRIBUTION TO PLATE HEIGHT

Mobile phase, flow-rate, and injection volume as in Table I.

Concentration injected (mM)	d_p = 10 μm*				d_p = 50 μm**			
	k'	H_{tot} (μm)	$H_{non\text{-}binding}$ (μm)	$H_{kinetic}$ (μm)	k'	H_{tot} (μm)	$H_{non\text{-}binding}$ (μm)	$H_{kinetic}$ (μm)
0.1	10.0	800	120	680	11.4	4050	2440	1610
0.2	9.5	820	120	700	10.6	4280	2420	1860
0.4	8.6	1180	120	1060	9.7	5400	2410	2990
0.6	8.1	1620	120	1500	9.2	4710	2400	2310
0.8	7.6	2100	120	1980	8.4	5630	2380	3250
1.0	7.3	2420	120	2300	8.0	6090	2370	3720

* Column: 5 cm × 0.5 cm I.D., 27 mg/g Con A, 10 μm, pore diameter 50 nm.
** Column: 3.0 cm × 0.3 cm I.D., 38 mg/g Con A, 50 μm, pore diameter 42 nm.

isotherm non-linearity and nature of the solute sugar on the apparent dissociation rate constant.

The apparent heterogeneous dissociation rate constant of the Con A–pNp-mannoside was determined on both the 10- and 50-μm particle supports over an injected concentration range of 0.1 to 1.0 m*M*. These results are shown in Fig. 3 and Table III. In Table IV, both the association rate constants, k_a, and the dissociation rate constants are listed as determined using the 10-μm support. The k_a values were evaluated using eqn. 2 with the phase ratio equal to N^0_{CA}/V_m where N^0_{CA} is the number of active moles of Con A in the column as determined from the isotherm measurements. The chromatographically determined value of k_a is somewhat less accurate than the corresponding k_d value due to the additional uncertainty associated with the measurement of N^0_{CA} and V_m.

Reference to Fig. 3 reveals several important points. First, note that the difference between the apparent dissociation rate constants as determined on the two different particle size supports at the same concentration is small, especially at low concentrations of pNp-mannoside. This agreement implies that the method used to determine $H_{kinetic}$, and hence k_d, is valid since $H_{kinetic}$ is the only plate height contribution which is independent of particle diameter. Secondly, Table III shows that the previously described decrease in K with increasing concentration of injected sugar arises from a decrease in both k_a and k_d, with the larger relative decrease in k_a accounting for the lower values of K at higher concentrations. Finally, at all concentrations examined, the apparent heterogeneous rate constants, k_a and k_d, are still approximately 10–20 fold lower than their solution phase counterparts. The decrease in k_d upon immobilization is greater than the decrease in k_a. The underlying reasons for the decrease in complex association and dissociation rates upon immobilization are unclear at this time. Such effects are not uncommon and are frequently observed with immobilized enzymes[18,19]. The reasons most often cited for changes in kinetic properties upon immobilization of a ligand include geometric factors and chemical factors related to the microenvironment at the surface. The reduced dimensionality

TABLE IV

APPARENT ASSOCIATION AND DISSOCIATION RATE CONSTANTS OF pNp-MANNOSIDE

All chromatographic conditions as in Table II. k_a calculated using eqn. 2 with $\varphi = 2.76 \cdot 10^{-4}$ M. $K = k_a/k_d$.

Concentration injected (mM)	k'	$k_a \cdot 10^{-4}$ $(M^{-1}\,s^{-1})$	k_d (s^{-1})	$K \cdot 10^{-4}$ (M^{-1})
0.1	10.0	1.16	0.32	3.62
0.2	9.5	1.14	0.33	3.44
0.4	8.6	0.72	0.23	3.11
0.6	8.1	0.50	0.17	2.93
0.8	7.6	0.39	0.14	2.75
1.0	7.3	0.32	0.12	2.64

concept, as developed by Astumian and Schelly[20], is probably not the reason for the decreased heterogeneous k_d observed here. Reduced dimensionality is predicted to cause a large decrease in rate constants only when the incoming solute is much larger than the immobilized ligand. In the case described here, the immobilized Con A is very large relative to the solute sugar, and reduced dimensionality predicts only very small effects on k_d. However, other steric factors related to inaccessibility of the Con A binding site due to immobilization cannot be excluded. The existence of a hydrophobic microenvironment at the surface may be related to the decrease in k_d as immobilized Con A has been shown to bind various small hydrophobic (non-sugar) molecules[21]. Whatever process is responsible for the observed decrease in the heterogeneous rate constants, the results of our studies indicate that this process does not affect the thermodynamics of the heterogeneous interaction, thus both k_a and k_d are nearly equally decreased.

The effect of isotherm non-linearity on the determination of the apparent rate constants using eqn. 2, as reflected in the concentration dependent rate parameters, is two-fold. First, k' is observed to decrease with increasing sugar concentration; a direct manifestation of isotherm non-linearity. Secondly, the system non-linearity will produce an additional contribution to band-broadening, $H_{\text{non-linear}}$, which is of course not included in the linear model of Horváth and Lin. This extra non-linear contribution to H is unaccounted for primarily because no satisfactory quantitative theory describing the effect of non-linearity on peak width is readily available as yet. The large increase in plate height, H_{total}, in Table III observed on the 10-μm particle support at sugar concentrations greater than 0.2 mM is predominantly due to the plate height contribution arising from isotherm non-linearity. In calculating k_d via eqn. 2, the increase in plate height due to non-linearity is partially offset by the decrease in k' arising from the same effect. Note, however, that the effect of isotherm non-linearity on k_d must be larger than its effect on k' because of the quadratic weighting in the second moment, from which k_d is derived, and the linear weighting in the first peak moment, from which k' is obtained. At low sample concentrations, the effects of isotherm non-linearity are minimized as much as possible within the constraints of the detection system used. At pNp-mannoside concentrations less than or equal to 0.2 mM, there is very little variation in the calculated rate constants with concentration, and the values of k_d obtained on the 10- and 50-μm particle supports

TABLE V

APPARENT RATE CONSTANTS OF pNp-GLUCOSIDE

All chromatographic conditions as in Table II. k_a and K determined as described in Table IV.

Concentration injected (mM)	k'	H_{tot} *(μm)*	$H_{non\text{-}binding}$ *(μm)*	$H_{kinetic}$ *(μm)*	k_d (s^{-1})	$k_a \cdot 10^{-3}$ $(M^{-1}\,s^{-1})$	$K \cdot 10^{-3}$ (M^{-1})
0.01	1.53	487	120	367	1.7	9.6	5.5
0.05	1.52	522	120	402	1.6	8.7	5.5
0.10	1.31	504	120	384	1.7	8.0	4.8
0.20	1.25	564	120	444	1.5	6.6	4.5

are in good agreement. Thus, we feel that the rate parameters obtained at low sample loadings adequately reflect the kinetic characteristics of silica-bound Con A, though due to the non-linearity of the system, these values should be regarded as apparent rate parameters since they are not strictly rate constants.

The apparent dissociation rate constant of the Con A–pNp-glucoside complex was also determined by measurement of the first and second peak moments and use of eqn. 2 (see Table V). Because pNp-glucoside is less retained on these columns, and its plate height is much smaller than pNp-mannoside, it is possible to use lower concentrations of this sugar and still obtain a signal-to-noise ratio which will allow precise moments analysis. The values listed in Table V show that the dissociation rate constant of pNp-glucoside is approximately five times larger than the dissociation rate constant of pNp-mannoside, consistent with the fact that, in solution, the relative affinity of Con A for a given sugar is determined by the lifetime of the complex, *i.e.*, magnitude of the dissociation rate constant, since the k_a values are relatively independent of sugar[17]. The much larger value obtained for the apparent k_d of pNp-glucoside, as compared with pNp-mannoside, unequivocally indicates that the process dominating the plate height in this system is chemical in nature and not related to slow solute diffusion in the stagnant mobile phase or in the surface protein layer (since the diffusional characteristics of these two sugars are identical). In addition, one can calculate the "film" diffusion coefficients which would be necessary to produce the very large plate heights observed in this system using the classical film diffusion equation:

$$H = \frac{2k' d_f^2 u}{3(1 + k')^2 D_s} \tag{10}$$

Using $H_{kinetic}$, k' and u values typical of our system, and a value of d_f representing the largest dimension of one Con A tetramer, the resulting value of D_s is on the order of 10^{-14} to 10^{-13} cm²/s. This is clearly an absurdly low value, especially when one compares it to the diffusion coefficient of phenol in weakly cross-linked swollen rubber, 10^{-8} cm²/s, which is a good model of a hydrated protein layer[22]. This calculation further supports the conclusion that the plate height in this system is dominated by slow chemical kinetics, and not other mass transfer processes. The relative magnitude of the apparent k_d values of these two sugars, in conjunction with the lower k' of pNp-glucoside, also indicates that at these low concentrations (< 0.1 mM injected in

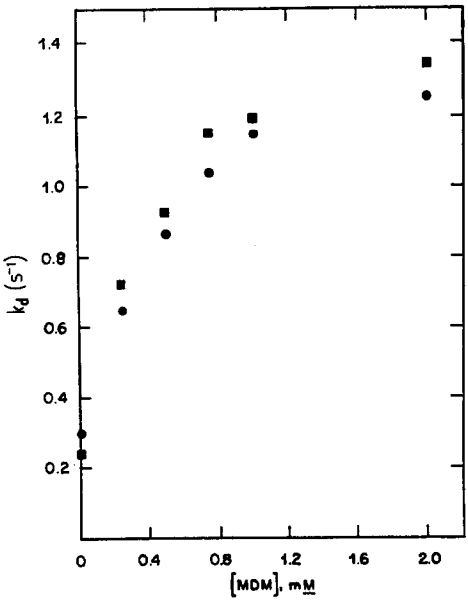

Fig. 4. Effect of competing sugar (S_2) on the apparent dissociation rate constant of the injected sugar (S_1). Column: 5.0 cm × 0.5 cm I.D., 29 mg/g Con A, 10 μm, pore diameter 50 nm. Mobile phase and flow-rate as in Fig. 2. Injection volume: 25 μl. ●, S_1 = 0.1 m*M* pNp-mannoside; ■, S_1 = 0.2 m*M* pNp-mannoside, S_2 = MDM.

each case), the effects of isotherm non-linearity on the determination of k_d are quite small at the lowest sugar concentration used herein.

Effect of competing sugar on the apparent dissociation rate and HPLAC efficiency

In our previous work, we reported on the effect of various concentrations (0 to 10 m*M*) of mobile phase competing sugar on the apparent dissociation rate constant of pNp-mannoside. These studies are extended here to include higher concentrations of competing sugar as well as other monovalent carbohydrates.

The effect of various concentrations (0 to 2.0 m*M*) of mobile phase MDM on the apparent dissociation rate constant of 0.1 m*M* pNp-mannoside is shown in Fig. 4. Table VI provides the effect of MDM on k' and H_{total} as well. The apparent dissociation rate constant varies linearly with the mobile phase concentration of competing MDM up to a concentration of 1.0 m*M*. At 2.0 m*M* competing sugar concentration, the curve levels off. Results obtained for the injection of 0.2 m*M* pNp-mannoside are also shown in Fig. 4 and the slopes of the k_d *vs.* [MDM] plot for the two concentrations of pNp-mannoside are not statistically different (900 ± 60 s^{-1} M^{-1}) indicating that isotherm non-linearity is not a significant factor in these results.

The effect of mobile phase competing sugar on the apparent dissociation rate constant of pNp-glucoside was not as clear as the effect on pNp-mannoside due to the inaccuracies involved in calculating k_d for k' less than 1.0. A decrease in k_d of pNp-glucoside was observed upon increasing the mobile phase concentration of MDM from 0 to 0.25 m*M*, but there was no consistent trend in k_d for MDM greater than 0.25 m*M*.

TABLE VI

EFFECT OF MOBILE PHASE COMPETING SUGAR ON THE CHROMATOGRAPHIC PROPERTIES OF pNp-MANNOSIDE

Column: 5.0 cm × 0.5 cm I.D., 29 mg/g Con A, 10 μm, pore diameter 50 nm. Solute: 25 μl of 0.1 m*M* pNp-mannoside. Flow-rate and mobile phase as in Table I.

Chromatographic parameter	*Concentration of MDM in the mobile phase (mM)*					
	0	*0.25*	*0.50*	*0.75*	*1.0*	*2.0*
k'	11.28	3.35	1.99	1.55	1.53	1.06
H_{tot} (μm)	824	863	817	732	673	648
k_d (s^{-1})	0.29	0.65	0.86	1.04	1.15	1.25

In an attempt to better understand the effect of competing sugar on the apparent dissociation rate constant of pNp-mannoside, a limited number of experiments were performed using MDG as the competing sugar. The results are shown in Table VII. At mobile phase concentrations of MDG greater than 2 m*M*, *i.e.*, 4 and 5 m*M*, the effect of MDG on k_d remains constant as in the case of MDM at concentrations greater than 1.0 m*M*. Although the scatter of the data is somewhat worse in this case than for the results shown in Table VI and Fig. 4, it is clear that the effect of MDG on the dissociation rate constant of pNp-mannoside is substantially less than the effect of MDM, *i.e.*, it takes more MDG than MDM to achieve the same reduction in k_d. The slope of the [MDG] *vs.* k_d line is roughly 200 s^{-1} M^{-1}, significantly less than the slope observed for MDM, approximately 900 s^{-1} M^{-1}. The decrease in slope is consistent with the relative binding constants of MDG and MDM to immobilized Con A as determined chromatographically by the equilibrium binding experiments ($0.16 \cdot 10^4$ and $0.7 \cdot 10^4$ M^{-1}, respectively). Since the forward rate constant for the two sugars is essentially the same in solution[23], the decrease in slope also parallels the difference in k_d of the two sugars. The variation in slope with the binding constant of the competing sugar indicates that the primary effect of competing sugar on k_d is chemical in nature and not simply a physical effect such as a diffusion process.

In Fig. 5, a plot of k_d *vs.* $1/k'$ for the two competitors is presented. Note that all points are clustered around a single line and that the deviation from the line for

TABLE VII

EFFECT OF MDG ON THE CHROMATOGRAPHIC PROPERTIES OF pNp-MANNOSIDE

Column, mobile phase, flow-rate and injection volume as in Table VI.

Chromatographic parameter	*Concentration of MDG in the mobile phase (mM)*			
	0	*0.5*	*1.0*	*2.0*
k'	11.28	4.39	3.11	2.13
H_{tot} (μm)	824	1320	946	987
k_d (s^{-1})	0.29	0.33	0.59	0.66

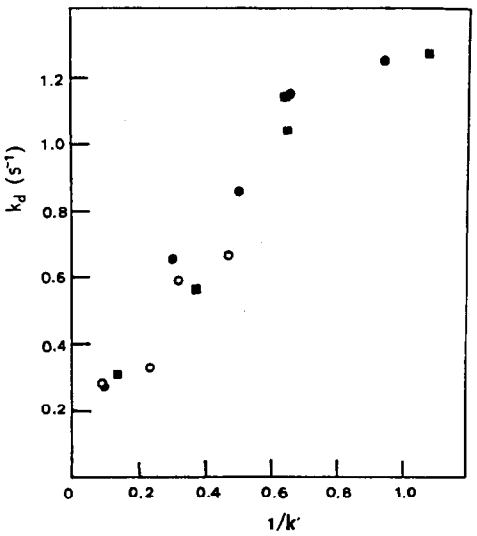

Fig. 5. Relationship between k' and apparent dissociation rate constants for S_2 = MDM and S_2 = MDG. ●,S_2 = MDM, column and conditions as in Fig. 4. ○, S_2 = MDG, column and conditions as in Fig. 4. ■, S_2 = MDM, column and conditions identical to the 10-μm column and conditions of Fig. 3.

the points due to MDG is not worse than the deviation for replicate experiments using MDM. The importance of this plot is that it demonstrates that the effect of competing sugar on k_d of the injected sugar arises primarily from its effect on k' and that the predominant effect of S_2 is to block accessible Con A binding sites.

The effect of (mobile phase) competing sugar on the apparent dissociation rate constants is surprising in light of the fact that solution phase studies by Lewis *et al.*[16] and by Farina and Wilkins[17] indicate that the dissociation rate of pNp-mannoside from soluble Con A is unaffected by the presence of a competitor. This discrepancy between the solution phase and heterogeneous cases has not yet been adequately explained. In several cases, the dissociation rate of the complex formed between Con A and multivalent ligands, *i.e.*, glycoproteins[24] and cell surfaces[25] was found to increase with competing sugar. These observations, however, should not be confused with the results reported here where the binding ligand is strictly monovalent. The enhanced rate in the multivalent case is easily explained in terms of multiple linkages with Con A and the blockage of vacant sites by the competing sugar. The apparent enhancement in the rate of dissociation of the injected sugar by the presence of a competing sugar in the heterogeneous case (two phase), as contrasted with the solution phase case, will be discussed in terms of three possible explanations: (1) ternary complex formation, (2) isotherm non-linearity and (3) inapplicability of the simple rate law used by Horváth and Lin.

The results reported here seem to suggest that (by analogy to the solution phase studies), that in the heterogeneous case, S_2 forms an intermediate ternary complex with S_1 which more readily dissociates to liberate S_1 than does the simple Con A–S_1 complex. The proposed mechanism can be schematically diagrammed as follows:

$$S_2 + PS_1 \underset{k'_{-1}}{\overset{k'_1}{\rightleftarrows}} S_1\text{–}P\text{–}S_2 \xrightarrow{k'_d} PS_2 + S_1 \tag{11}$$

In eqn. 11, and in all of those which follow, P refers to the immobilized Con A, S_1 refers to the injected sugar, S_2 refers to the competing sugar and k'_d refers to the intrinsic rate constant for the dissociation of the ternary complex. k_d always refers to the intrinsic dissociation rate constant of the binary complex.

In accordance with mechanism 11, the appearance of S_1 is given by the rate law:

$$\frac{d[S_1]}{dt} = k'_d\,[S_1\text{–}P\text{–}S_2] \tag{12}$$

The concentration of the intermediate species S_1–P–S_2 can be expressed in terms of the rate constants for the reversible formation of this species:

$$[S_1\text{–}P\text{–}S_2] = \frac{[S_2]\,[PS_1]\,k'_1}{(k'_d + k'_{-1})} \tag{13}$$

In deriving eqn. 13, it was assumed that the steady state approximation on $[S_1$–P–$S_2]$ was valid, *i.e.*, $d[S_1\text{–}P\text{–}S_2]/dt = 0$. The equilibrium constant for the initial phase of the reaction, $k_{eq} = k'_1/k'_{-1}$, was not used to obtain the concentration of S_1–P–S_2 because it is unlikely that equilibrium exists in this case due to the small value of k'_{-1}. Eqn. 13 still encompasses the equilibrium case. The rate of production of S_1 in the presence of S_2 is therefore:

$$\frac{d[S_1]}{dt} = k_d[PS_1] + \frac{k'_d k'_1[S_2]\,[PS_1]}{(k'_{-1} + k'_d)} \tag{14}$$

Thus, the observed rate constant, $k_{d,obs}$, in the presence of S_2 is equal to $k_d + k'_d k'_1[S_2]/(k'_{-1} + k'_d)$. The results of this simple kinetic analysis correlate with the observation that the rate enhancement is proportional to the concentration of competing sugar. In addition, the slope of the $k_{d,obs}$ *vs.* $[S_2]$ plot is predicted to be equal to $k'_d k'_1/(k'_d + k'_{-1})$. The nature of the competing sugar, *i.e.*, MDM or MDG also plays a role in determining the slope since k'_1 and k'_{-1} are the rate constants representing the interaction of Con A with S_2.

Although all literature reports indicate that each Con A monomer contains a single biospecific sugar binding site accommodating a single carbohydrate, most reports also indicate that each Con A monomer contains a distinct non-biospecific hydrophobic binding site[26]. One physical explanation which may be consistent with the ternary complex formation involves the participation of both the biospecific and hydrophobic sites in ternary complex formation. It is likely that the binding of the hydrophobic sugar, pNp-mannoside, involves interaction at both the carbohydrate and hydrophobic sites. The incoming, less hydrophobic sugar, S_2, could then displace S_1 at the carbohydrate site, while S_1 remains attached, at least transiently, to Con A via interaction of its *p*-nitrophenyl moiety at the hydrophobic site. The second step of S_1 dissociation, as represented by k'_d, would be the slow step of desorbing from

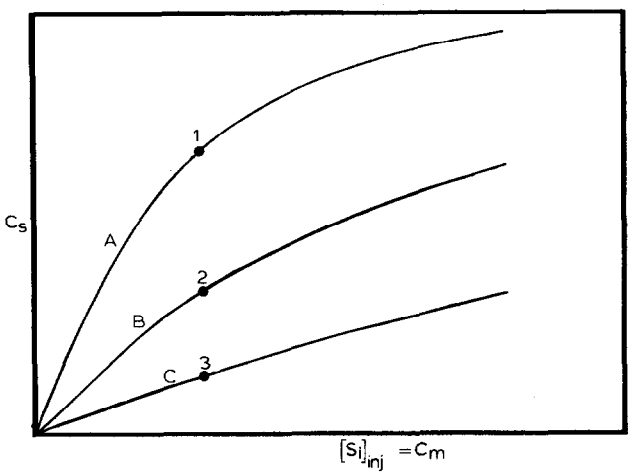

Fig. 6. Hypothetical isotherms of S_1 on Con A-silica in the presence of competing mobile phase sugar. Isotherm A, $[S_2]_A = 0$; isotherm B, $0 < [S_2]_B < [S_2]_C$; isotherm C, $[S_2]_C > [S_2]_B$.

the hydrophobic site. The role of S_2 in this process is to promote the dissociation of S_1 by removal of the first biospecific interaction and then by "crowding out" S_1 once it is involved in only the hydrophobic attachment. This two step mechanism of hydrophobic sugar interaction derives some indirect support from solution phase studies. For the series of the increasingly hydrophobic sugars, MDM, pNp-mannoside and 4-methylumbelliferyl-α-D-mannoside, the increase in hydrophobicity is accompanied by an increase in the binding constant due primarily to the decrease in the k_d values[16,17,23]. The trends are similar for the glucose derivatives. Thus, the hydrophobic portion of the carbohydrate molecule controls the variation in the dissociation constant. Also in support of this hypothesis is the enhancement effect of ethylene glycol on the dissociation rate of pNp-mannoside[6]. Since the usual effect of ethylene glycol is to reduce the strength of hydrophobic interactions, the increased k_d in the presence of ethylene glycol implies that the hydrophobic component of the interaction between pNp-mannoside and immobilized Con A is very important in establishing the dissociation rate.

The second possible explanation for the differing effects of competing sugar on k_d in the homogeneous and heterogeneous cases arises from the problem of isotherm non-linearity. This effect is most easily explained by reference to the isotherms shown in Fig. 6. These isotherms were generated by using simple equilibrium calculations to describe the effect of $[S_2]$ on the amount of S_1 bound to the immobilized Con A at a given concentration of injected S_1. The values of K_1, K_2, N^0_{CA} and $[S_1]_{total}$ used to generate these isotherms were typical values for the HPLAC system investigated here. At higher values of c_m (not shown in Fig. 6) the isotherms coincide at a c_s value limited by the total amount of Con A in the column. Imagine first that, in the absence of competing sugar, the relative amount of S_1 injected corresponds to point 1 on isotherm A. Point 1 is clearly in the non-linear region of this isotherm. As mobile phase competing sugar is added, isotherm B is now in effect and point 2 on isotherm B is in a more linear region than point 1 on isotherm A. Finally, additional competing

sugar is represented by point 3 on isotherm C which is well into the linear region of the isotherm. Additional peak broadening is concomitant to isotherm non-linearity. As the experiment progresses from isotherm A to isotherm C in Fig. 6, the non-linear contribution to H progressively increases. Since there is no quantitative theory available to predict the effects of isotherm non-linearity on H, we chose to ignore these effects and to carry out the experiments at the lowest possible concentrations in hope of minimizing these effects. Thus, the result of ignoring the non-linear contribution to H is to overestimate the value of k_d at a given value of k'. The relative error due to the over-estimation of H_{kinetic} becomes progressively worse as the non-linearity increases. In summary then, the value of k_d would be observed to increase as we move to more linear isotherms by adding competing sugar.

Mathematically, this effect arises out of the assumptions used by Horváth and Lin in formulating the H_{kinetic} term. Recall from the introduction that the simple model used in deriving H_{kinetic} was based on the assumption that only a negligibly small fraction of the available ligands were complexed with solute. The simple kinetic law used by Horváth and Lin to express the time dependence of the concentration of bound solute can be expressed in terms of the production of mobile phase sugar for the case examined here as follows:

$$\frac{d[S_1]}{dt} = k_d[PS_1] - k_a[S_1]\,[P] \tag{15}$$

Under conditions of competing sugar in the mobile phase, however, the surface concentration of Con A is not constant and consequently is a function of time. This is precisely the unsolved problem of non-linear kinetics in a general theory of chromatography, so it is impossible to mathematically predict the effect of the change in the concentration of free Con A on the calculated k_d. It is possible that the competitor will interact with P in such a fashion that the apparent k_d would vary with competing sugar.

Due to the mathematical complexities involved with non-linear kinetics, the above explanation can only be verified by performing the experiment at very, very low concentrations of injected sugar so that the isotherm region explored is truly linear. Under these conditions, k_d should be independent of the concentration of competing sugar if in fact the apparent increase in k_d is due to the isotherm non-linearity.

In spite of our inability to experimentally test this hypothesis, we can set a limit on the non-linear effect on k_d. It is obvious that, although the increased isotherm linearity will serve to increase k_d, the effect cannot be greater than that observed for the most linear portion of the isotherm in the absence of competing sugar. The greatest effect that isotherm non-linearity could have then, will be to increase k_d to the value that it would have when the concentration of injected sugar, S_1, is equal to zero. Extrapolation of the k_d *vs.* concentration injected curve of Fig. 3 to $[S_1] = 0$ shows that the limiting value of k_d cannot possibly be greater than 0.5 s^{-1}. Thus, the greatest possible effect of isotherm non-linearity on k_d would be to increase it to 0.5 s^{-1} and this is significantly lower than the value of 1.25 s^{-1} observed in the presence of 1.0 m*M* MDM

Some experimental support for the minimal effect of isotherm non-linearity on

k_d comes from the close agreement (at low concentrations of S_1) in the k_d values determined on the 10- and 50-μm supports (see Fig. 3). On the 50-μm particle support, the mass transfer broadening and concomitant dilution effects are significantly greater than on the 10-μm support, so that the isotherm non-linearity is expected to persist to much lower values of mobile phase solute concentration on the 50-μm support. Therefore, even with the difference in the degree of isotherm non-linearity at a given concentration of S_1, the good agreement noted for k_d on these two supports shows that isotherm non-linearity cannot be a major contributing factor to the variation of k_d with $[S_2]$. Furthermore, parallel plots of the apparent dissociation rate constant *vs.* $[S_2]$ at two different concentrations of injected sugar, S_1, also strongly substantiate the view that the variation in $k_{d,obs}$ with $[S_2]$ is not an artifact of isotherm non-linearity. In essence then, the non-linear isotherm does contribute somewhat to the observed k_d results, but it is a limited contribution and cannot possibly account for the total increase in k_d noted here.

The final explanation of the dependence of k_d on the concentration of mobile phase competing sugar again involves our use of the simple kinetic model of Horváth and Lin in deriving $H_{kinetic}$ for a more complex situation. Recall from the introduction that the binding of the injected sugar to immobilized Con A is represented in the Horváth and Lin theory by the simple, reversible process shown in eqn. 3. Under the chromatographic conditions of competing sugar in the mobile phase, however, the binding/debinding process is more realistically represented by the coupled, consecutive reactions shown below:

$$PS_1 \underset{k_a}{\overset{k_d}{\rightleftarrows}} P + S_1 \tag{16}$$

$$P + S_2 \underset{k_{d,2}}{\overset{k_{a,2}}{\rightleftarrows}} PS_2 \tag{17}$$

The rate law describing the chromatographic case must include the back reaction (represented by k_a) in eqn. 16 since the free P is not immediately and quantitatively bound by S_2. The rate law describing the chromatographic situation can be formulated by beginning with the following restatement of eqn. 7:

$$\frac{d[PS_1]}{dt} = k_a[S_1]\,[P] - k_d[PS_1] \tag{18}$$

The concentration of P in eqn. 18 is a function of both the concentration of S_2 present as well as the rate constants for the Con A–S_2 interaction. The rate law, eqn. 18, can be expressed in terms of $[S_2]$ and $[PS_2]$ by invoking the steady-state approximation and assuming that the concentration of free P does not change significantly during the course of the reaction, *i.e.*, $d[P]/dt = 0$. Then:

$$\frac{d[P]}{dt} = 0 = k_d[PS_1] + k_{d,2}[PS_2] - k_a[P][S_1] - k_{a,2}[P]\,[S_2] \tag{19}$$

Eqn. 19 can then be solved for [P] and this expression can be used in eqn. 18 to finally obtain:

$$\frac{d[PS_1]}{dt} = \left\{k_a[S_1]\left(\frac{k_d[PS_1] + k_{d,2}[PS_2]}{k_a[S_1] + k_{a,2}[S_2]}\right)\right\} - k_d[PS_1] \tag{20}$$

As shown above, then, the observed rate constant is not simply the intrinsic rate constant k_a as measured in the absence of sugar, but it is a function of the concentrations of free S_1, S_2, PS_1 and PS_2, and the associated rate constants. The discussion here is presented in terms of k_a for simplicity. Note that an equivalent effect on k_d can be obtained by the relationship of eqn. 2. Physically, the effect of S_2 is to decrease the amount of P available for binding to S_1 (or, in the column; re-binding). Hence, the relative contribution of the back reaction of eqn. 16 decreases as the amount of S_2 is increased. The total reaction scheme cannot be interpreted within the constraints of the Horváth and Lin formalism since [P] is not constant as $[S_2]$ is varied. That is, in the Horváth and Lin formalism, it is assumed that the total amount of P is vastly greater than the amount of S_1 in the column. Simple extension of their model to preserve its linear nature requires that $[S_2] \ll [P]$ which is decidedly not the case in this work.

In terms of the Horváth and Lin general plate height equation, the kinetic phenomenon responsible for H_{kinetic} is represented by eqn. 18 and thus the rate constant extracted by the use of eqn. 2 refers to an intrinsic rate constant only in the case where the heterogeneous reaction can be described by the simple one step reversible binding of eluite. Including the effect of S_2 on P via the coupled consecutive reaction scheme shown in eqns. 16 and 17 would lead to enormous mathematical difficulties in the solution of the mass balance equations. Thus, the Horváth and Lin equation for k_d provides the intrinsic rate constant only in the absence of competing sugar. As $[S_2]$ is increased, the approximation made by our use of the Horváth and Lin equation becomes increasingly worse. In the case of a huge excess of competing sugar, the free Con A is immediately and quantitatively bound by S_2 and the rate law describing this situation is simply:

$$\frac{d[PS_1]}{dt} = -k_d[PS_1] \tag{21}$$

This situation probably occurs in the region where the k_d *vs.* $[S_2]$ curve levels off.

Although this final hypothesis may adequately explain the k_d dependence on S_2, it is experimentally untestable and thus its applicability is difficult to evaluate. It may be argued that the changes in rate law prevailing at the different levels of mobile phase competing sugar are irrelevant, since the primary effect of S_2 is to decrease the apparent phase ratio and that this decrease is reflected in the change in k' with $[S_2]$ (and therefore adequately accounted for in the Horváth and Lin equation). Due to insurmountable mathematical difficulties, however, it is impossible to see if the effect of S_2 is solely in the value of k'.

This rather long discussion of the possible explanations for the observed difference in the effect of S_2 on k_d in the homogeneous *vs.* heterogeneous cases has been included here to emphasize the complexity of the situation and the need for a better

theoretical foundation for HPLAC. Note that, mathematically, the coupled consecutive reaction scheme is similar to the effects of isotherm non-linearity. In both cases, the Horváth and Lin model fails to account for the variation in rate with competing sugar because the decrease in available ligand, P, is not considered other than via the effect of S_2 on the effective equilibrium binding constant for S_1. Due to inadequate chromatographic theory in the case of non-linear or complex kinetics, and to experimental limitations, none of the possibilities described here can be totally excluded at this time.

CONCLUSIONS

Further studies on the thermodynamic and kinetic properties of silica-bound Con A have shown that, while the thermodynamic properties of the Con A–sugar interaction are largely unaffected by immobilization, the kinetic parameters of the interaction are substantially reduced. The chromatographic determination of binding constants is complicated by the very non-linear isotherm of this system. The use of the Horváth and Lin general plate height equation to determine the rate constants is also affected by the non-linearity of the system, but experiments at low sample loadings produce reasonable estimates of the rate parameters characterizing the heterogeneous system. Addition of mobile phase competing sugar causes an increase in the chromatographically determined rate constants. This effect is not observed in solution phase studies. The reasons for this anomalous heterogeneous behavior include (1) the formation of a ternary complex in the heterogeneous case or (2) the limitations of the Horváth and Lin equation when applied to the system containing mobile phase competing sugar. Isotherm non-linearity may be a contributing factor, but cannot totally account for the observed behavior.

These studies have shown that the limitations of this HPLAC system are set by the sluggish chemical kinetics of the Con A–sugar interaction, and not by any mass transfer related effects. The solutes examined here are univalent with respect to their biospecific interactions with Con A. Studies using glycoproteins as solutes have shown that the desorption rates of multivalent solutes are significantly slower than those described here[27]. Since many biological interactions have rate constants similar to those of the Con A–sugar interaction, and since these rate constants may be further reduced upon immobilization, sluggish kinetics may limit the analytical utility of many HPLAC systems.

ACKNOWLEDGEMENTS

Financial support for A.J.M. was provided by a fellowship from Dow Chemical Corporation and by the National Science Foundation (CHE 8217363).

REFERENCES

1 P.-O. Larsson, M. Glad, L. Hansson, M.-O. Mansson, S. Ohlson and K. Mosbach, *Adv. Chromatogr. (N.Y.)*, 21 (1983) 41.
2 V. Kasche and B. Galunsky, in T. Gribnau, J. Visser and R. Nivard (Editors), *Affinity Chromatography and Related Techniques*, Elsevier, Amsterdam, 1982, p. 93.
3 V. Kasche, K. Buchholz and B. Galunsky, *J. Chromatogr.*, 216 (1981) 169.

4 R. R. Walters, *J. Chromatogr.*, 249 (1982) 19.
5 F. Arnold, *Ph.D. Dissertation*, University of California, Berkeley, CA (1985).
6 A. J. Muller and P. W. Carr, *J. Chromatogr.*, 284 (1984) 33.
7 Cs. Horváth and H.-J. Lin, *J. Chromatogr.*, 149 (1978) 43.
8 Cs. Horváth and H.-J. Lin, *J. Chromatogr.*, 126 (1976) 401.
9 B. Cunningham, J. Wang, M. Pflumm and G. Edelman, *Biochemistry*, 11 (1972) 3233.
10 M. Broquaire, *J. Chromatogr.*, 170 (1979) 43.
11 R. Gray and R. Glew, *J. Biol. Chem.*, 248 (1973) 7547.
12 K. Takeo, in T. Bog-Hansen (Editor), *Lectins —Biology, Biochemistry, Clinical Biochemistry*, Vol. II, Walter de Gruyter, Berlin, 1982, p. 583.
13 W. Bessler, J. Shafer and I. Goldstein, *J. Biol. Chem.*, 249 (1974) 2819.
14 M. Dani, F. Marca and G. Rialdi, *Biochim. Biophys. Acta*, 667 (1981) 108.
15 C. Brewer, D. Marcus, A. Grollman and H. Sternlicht, in E. F. Osserman, R. E. Canfield and S. Beychok (Editors), *Lysozyme*, Academic Press, New York, 1974, p. 239.
16 S. Lewis, J. Shafer and I. Goldstein, *Arch. Biochem. Biophys.*, 172 (1976) 689.
17 R. Farina and R. Wilkins, *Biochim. Biophys. Acta*, 631 (1980) 428.
18 P. Carr and L. Bowers, *Immobilized Enzymes in Analytical and Clinical Chemistry*, Wiley-Interscience, New York, 1980, p. 155.
19 Y. Lee, K. Wun and G. Tsao, in H. H. Weetall and S. Suzuki (Editors), *Immobilized Enzyme Technology*, Plenum, New York, 1974, p. 129.
20 R. Astumian and Z. Schelly, *J. Am. Chem. Soc.*, 106 (1984) 304.
21 A. Bergold and P. Carr, *Minnesota Chromatography Forum, Minneapolis, May 21, 1985*, Paper No. 38.
22 B. Karger, L. Snyder and Cs. Horváth, *An Introduction to Separation Science*, Wiley-Interscience, New York, 1973, p. 81.
23 R. Clegg, F. Loontiens, A. Van Landschoot and T. Jovin, *Biochemistry*, 20 (1977) 4687.
24 S. Podder, A. Surolia and B. Bachhawat, *Eur. J. Biochem.*, 44 (1974) 151.
25 P. Cuatrecasas, *Biochemistry*, 12 (1973) 1312.
26 K. Hardman and C. Ainsworth, *Biochemistry*, 12 (1973) 4442.
27 A. J. Muller and P. W. Carr, *J. Chromatogr.*, 294 (1984) 235.